

HT2012-58191

## CONCENTRATION DISTRIBUTION RESEARCH OF A SPECIAL DC PULVERIZED COAL BURNER AND RESISTANCE ANALYSIS

**Mo Yang**

College of Energy and Power Engineering,  
University of Shanghai for Science and Technology  
Shanghai, China

**Chunsun Guo**

College of Energy and Power Engineering,  
University of Shanghai for Science and Technology  
Shanghai, China

**Yuwen Zhang**

Department of Mechanical and Aerospace  
Engineering, University of Missouri  
Columbia, Missouri, USA

**Zhangyang Kang**

College of Energy and Power Engineering, University of  
Shanghai for Science and Technology  
Shanghai, China

### ABSTRACT

In this paper, a direct current (DC) anti-bias burner has been numerically simulated. This kind burner is combination of bias block and elbow bend and its bias block is located behind the bend. Effects of the bias block's angle and location on coal distribution in the burner export are investigated. Euler-Lagrange approach is employed to study the gas-solid two-phase flow. The gas-phase is simulated using the RNG  $k-\epsilon$  model and solid-phase is modeled using the discrete phase model (DPM). The results show that, installing a bias block behind the elbow can achieve a uniform distribution in outlet and the high concentrations region non-adherent. Relative to the location, the bias block angle changes is the main reason of generating resistance. When  $\alpha = 25^\circ$   $L = 150\text{mm}$ , the distribution of pulverized coal of the burner outlet is the most uniform and the resistance is not large, which could satisfy the good anti-bias effect and moderate resistance loss at the same time.

### INTRODUCTION

With the benefits of burning low volatile coal more efficiently and decreasing the NO<sub>x</sub> emissions, fuel rich-lean combustion technology has been widely developed and applied. However, the actual operation of the project in some cases need to avoid uneven distribution of pulverized coal in the burner export, such as the swirl burner, which distribution of pulverized coal in the export directly affects the coal combustion efficiency. In the combustion process, primary air

wraps around pulverized coal into the furnace to combustion and secondary air divides into inner and outer classification to go into. The uneven distribution of pulverized coal will affect the pulverized coal combustion atmosphere, thereby affecting NO<sub>x</sub> formation, reducing the efficiency of pulverized coal combustion [1]. The coal-fired boilers, which applied in ultra-supercritical power plant, adopt an incident mode of uniform concentration. It is required that the burner has a special structure to achieve such an effect. As the mills are arranged on one side of the boiler and boiler demands strictly tangential angle, the primary air is certain to pass the elbow bend, which leads to uneven distribution of export concentration. To solve this problem, this paper presents an anti-bias burner that combined the bias block and elbow; its bias block is located behind the bend. This structure can achieve coal concentration distribution in the export as even as possible [2].

Many scholars have studied the gas-solid flow characteristics in elbow bend. By experimental and numerical simulation methods, Zhou et al [3] have analyzed the effect on the separation characteristics of fuel rich-lean burner, made by the uneven distribution of mixture of pulverized coal and air after primary air flowed through the elbow. Using RNG  $k-\epsilon$  model and random trajectory model, Jing et al. [4] simulated the gas-solid flow by PISC algorithm of particles and fluid coupling. Bias block is used in a variety of industrial and power boiler burners. Pulverized coal concentration percussive adjustable burner adopts a structure of bias block and clapboard and through a large number of experiments and numerical

simulations. The concentration characteristics of this fuel rich-lean burner have been obtained and the characteristics of resistance have been analyzed [5]-[8]. Yan [9] installed bias block in the flow direction inside the rear of elbow bend, which strengthens the role of elbow bend in the concentration separation. Through simulation and experiments, they studied this structure application in engineering. However, the study of anti-bias combustion technology is relatively rare; this special pulverized coal burner will be numerically simulated in this paper. By changing the bias block's angle and location, the effect of bias block's structure on coal distribution in the burner export will be investigated.

## PROBLEM AND MATHEMATICAL MODEL

### Physical Model

As the model shown in Figure 1, the angle of bend is  $39^\circ$  and the bias block is installed in the pulverized coal rich side behind the bend. After the bias block, the burner into the furnace turns from a round cross-section into a square one. The entrance is round face, the export is square face, and the rest faces are walls. The angle between the flow direction (this article is horizontal direction) and the bias block windward,  $\alpha$ , represent the bias block's angle. L is the distance between the bias block and bend. With bias block's angle changing from  $15^\circ$  to  $35^\circ$  and L from 0 to 250mm, thirty different cases (shown in Table 1) have been numerically simulated. The cases without bias block are also simulated at the same time.

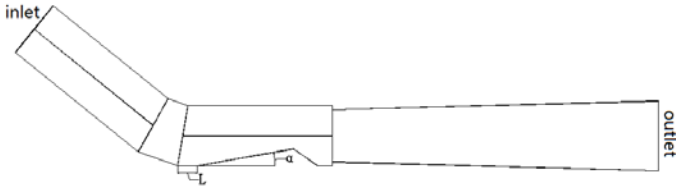


Fig.1 The structure of burner

Tab. 1 Simulation cases

$\frac{L}{\alpha}$	0mm	50mm	100mm	150mm	200mm	250mm
$15^\circ$	NO.1	NO.2	NO.3	NO.4	NO.5	NO.6
$20^\circ$	NO.7	NO.8	NO.9	NO.10	NO.11	NO.12
$25^\circ$	NO.13	NO.14	NO.15	NO.16	NO.17	NO.18
$30^\circ$	NO.19	NO.20	NO.21	NO.22	NO.23	NO.24
$35^\circ$	NO.25	NO.26	NO.27	NO.28	NO.29	NO.30

### Mathematical model

In this paper, Euler-Lagrange method is adopted in simulation. Solid-phase is simulated in discrete phase model (DPM) and the gas phase in RNG (renormalization group) k- $\epsilon$  model. In order to improve accuracy, the discretization of momentum equation, pressure equation, turbulent kinetic energy equation and turbulent dissipation equation is using Quick

scheme. The coupling of pressure and velocity adopts SIMPLE algorithm.

Discrete phase model is used in particle trajectories calculation.

### Gas phase

The general equation the RNG k- $\epsilon$  transport equation of is showed as follows [10]:

$$\begin{aligned} & \frac{\partial}{\partial t}(\rho_g \phi) + \frac{\partial}{\partial x}(\rho_g u \phi) + \frac{\partial}{\partial y}(\rho_g v \phi) + \frac{\partial}{\partial z}(\rho_g w \phi) \\ & = \frac{\partial}{\partial x}(\Gamma_\phi \frac{\partial \phi}{\partial x}) + \frac{\partial}{\partial y}(\Gamma_\phi \frac{\partial \phi}{\partial y}) + \frac{\partial}{\partial z}(\Gamma_\phi \frac{\partial \phi}{\partial z}) + S_\phi \end{aligned} \quad (1)$$

In this equation, corresponding content about  $\phi$  (common variable),  $\Gamma_\phi$  (transport coefficients) and  $S_\phi$  (source) is showed in Table 2 :

Tab.2 Parameters of general equation in RNG k- $\epsilon$  model

Equation	$\phi$	$\Gamma_\phi$	$S_\phi$
continuity	1	0	0
x-momentum	u	$\mu_e$	$-\frac{\partial p}{\partial x} + \frac{\partial}{\partial x}(\mu_e \frac{\partial u}{\partial x}) + \frac{\partial}{\partial y}(\mu_e \frac{\partial v}{\partial x}) + \frac{\partial}{\partial z}(\mu_e \frac{\partial w}{\partial x}) - \frac{2}{3} \frac{\partial}{\partial x}(\rho_g k)$
y-momentum	v	$\mu_e$	$-\frac{\partial p}{\partial y} + \frac{\partial}{\partial x}(\mu_e \frac{\partial u}{\partial y}) + \frac{\partial}{\partial y}(\mu_e \frac{\partial v}{\partial y}) + \frac{\partial}{\partial z}(\mu_e \frac{\partial w}{\partial y}) - \frac{2}{3} \frac{\partial}{\partial y}(\rho_g k)$
z-momentum	w	$\mu_e$	$-\frac{\partial p}{\partial z} + \frac{\partial}{\partial x}(\mu_e \frac{\partial u}{\partial z}) + \frac{\partial}{\partial y}(\mu_e \frac{\partial v}{\partial z}) + \frac{\partial}{\partial z}(\mu_e \frac{\partial w}{\partial z}) - \frac{2}{3} \frac{\partial}{\partial z}(\rho_g k)$
Turbulence Kinetic energy	k	$\frac{\mu_e}{\sigma_k}$	$G_k + G_b - \rho_g c_D \epsilon$
Turbulent kinetic energy dissipation rate	$\epsilon$	$\frac{\mu_e}{\sigma_\epsilon}$	$\frac{\epsilon}{\kappa} [c_1(G_k + G_b)(1 + c_3 R_f) - c_2 \rho_g \epsilon] - R_\epsilon$

The turbulent eddy viscosity is:

$$\mu_T = c_\mu \rho_g \kappa^2 / \epsilon \quad (2)$$

The effective viscosity is

$$\mu_e = \mu + \mu_T \quad (3)$$

Transport coefficient is defined as:

$$\Gamma_\phi = \mu / \sigma_\phi \quad (4)$$

where  $\sigma_\phi$  is Turbulent Prandtl number.

Average flow rate of turbulent kinetic energy produced is:

$$G_k = \mu_T [2(\frac{\partial u}{\partial x})^2 + 2(\frac{\partial v}{\partial y})^2 + 2(\frac{\partial w}{\partial z})^2 + (\frac{\partial u}{\partial y} + \frac{\partial v}{\partial x})^2 + (\frac{\partial v}{\partial z} + \frac{\partial w}{\partial y})^2 + (\frac{\partial w}{\partial x} + \frac{\partial u}{\partial z})^2] \quad (5)$$

The production rate of turbulent kinetic energy buoyancy is:

$$G_b = -\beta \rho_g (\mathbf{g}_x \frac{\mu_T}{\sigma_T} \frac{\partial T}{\partial x} + \mathbf{g}_y \frac{\mu_T}{\sigma_T} \frac{\partial T}{\partial y} + \mathbf{g}_z \frac{\mu_T}{\sigma_T} \frac{\partial T}{\partial z}) \quad (6)$$

The volume expansion coefficient is

$$\beta = \frac{1}{\rho_g} (\frac{\partial \rho_g}{\partial T})_p \quad (7)$$

The flux Richardson number is:

$$R_f = -G_b / G_k \quad (8)$$

and  $R_\varepsilon = [c_\mu \rho_g \eta^3 (1 - \eta / \eta_0) / (1 + \beta \eta^3)] (\varepsilon^2 / \kappa)$ , where  $\eta = (S\kappa) / \varepsilon$ ,  $S$  is the strain rate tensor,  $\eta_0 = 4.38$ ,  $\beta = 0.012$ .

*Particle motion equation:*

By integrating differential equations of particle force in lagrangian coordinates, track of the discrete phase particles can be solved. The form of particle force balance equation (Particle inertia= the sum of the various forces effecting on the particles) in the Cartesian coordinate system (in x- direction) is as follow:

$$\frac{du_p}{dt} = F_D(u - u_p) + \frac{\mathbf{g}_x(\rho_p - \rho)}{\rho_p} + F_x$$

where  $F_D(u - u_p)$  is the drag force per unit mass of particle

$$F_D = \frac{18\mu}{\rho_p d_p^2} \frac{C_D Re_p}{24}$$

$u_p$  is the velocity of particle,  $u$  is fluid phase speed,  $\mu$  is the molecular viscous of fluid,  $\rho$  is the density of particle,  $\rho$  is fluid density,  $d$  is the diameter of particle.  $Re_p$  is relative Reynolds number (particle Reynolds number), which is defined as:

$$Re_p \equiv \frac{\rho d_p |u_p - u|}{\mu}$$

Without considering the particle shape factor, when the particles are the same sphere, the traction coefficient  $C_D$  can be defined as:

$$C_D = a_1 + \frac{a_2}{Re_p} + \frac{a_3}{Re_p^2}$$

For spherical particles, when Reynolds number changes in a certain range,  $a_1$ ,  $a_2$ ,  $a_3$  are constants given by Morsi and Alexander [11].

### Boundary conditions

Continuous phase and coal particles enter the burner showed in Fig. 1 from the inlet of the tube and exit from the outlet.

- 1) Inlet condition: gas phase adopts the boundary of velocity inlet. Designating inlet velocity and modified turbulent viscosity. The turbulence intensity and the modified turbulent viscosity of inlet are calculated by following formulas.

$$I = 0.16(Re)^{-1/8}, \quad \tilde{\nu} = \sqrt{\frac{3}{2}} u I, \quad I = 0.07 L$$

where  $L$  is the characteristic length,  $Re$  is the Rayleigh number,  $I$  is the turbulence intensity,  $\tilde{\nu}$  is the modified turbulent viscosity, and  $u$  is the average speed of the inlet. Solid phase designates initial velocity and mass flow rate of the particles. Particles uniformly distributed at the entrance.

- 2) Wall condition: adopt standard wall functions at the near wall. No-slip boundary condition is adopted in wall. The particle phase is satisfied with the conditions of perfectly elastic collision without energy loss.
- 3) Outlet condition: gas phase adopts pressure outlet boundary condition. The outlet condition of particles phase is escape boundary.

### Assumptions

For the characteristics of this study, the actual characteristics of gas-solid flow are given full consideration. The following assumptions are made.

- (1) Particles are spherical shape.
- (2) Gas phase is Newtonian fluid and the two phase physical properties remain unchanged.
- (3) Flow is three-dimensional, steady, incompressible, and isothermal.
- (4) The impact from molecular diffusion and Brownian motion is not considered.
- (5) As the volume fractions of particles are smaller, the collision between particles can be ignored.
- (6) Consider the one-way coupling between gas and particle.
- (7) Do not consider particle breakage.

### Meshing

Through the simulation of grid with different orders of magnitude, the sensitivity of the grid-independent has been tested. Finally, it is determined to adopt 347,114 structured grids.

## RESULTS AND DISCUSSION

### Impact of bias block's angle

Figure 2 shows pulverized coal concentration distribution in the export of the six cases with bias block angle of  $0^\circ, 15^\circ, 20^\circ, 25^\circ, 30^\circ, 35^\circ$  ( $L = 150\text{mm}$ ). Obviously, without bias block, the pulverized coal distribution of the outlet appears rich-lean separation, the rich side of pulverized coal gets close to the outer wall and there is concentration core. The pulverized coal concentration shows a downward trend from the outer to the inner wall. Equipped with a bias block of small angle, the

coal distribution area becomes larger at the outlet, maximum concentration becomes smaller, and high concentration of pulverized coal region moves to the middle area. With the angle increasing, coal distribution gradually tends to be uniform. As bias block angle continues to increase, the distribution of coal gradually appears high concentration region and concentration core again, but compared to the situation without bias block, the high concentration area is located near the center of outlet. When the angle of bias block is 20°, the concentration distribution is most uniform and the anti-bias effect is best. Combined with burner structure, this result occurs because through the elbow bend, under the inertia and centrifugal force, most of the pulverized coal moves closely to the outer wall. Then through the bias block, the rich side of pulverized coal next to the wall is bumped by bias block and the flow direction deflects to the lean side. The rich side is turbulent mixed with the lean side. With different angle of bias block, the magnitude and direction of the impact force differs. When angle is small, the flow direction of the rich side of pulverized coal deflects a little, the mixture with the lean side is weak and anti-bias effect is not obvious. The larger angle bias block could strengthen the blend of the rich side and lean side, and pulverized coal concentration in the export becomes more and more even. When the angle increases larger to a certain degree, the flow area is reduced a lot after bias block, which is equivalent to a scaling structure, and the velocity of pulverized coal increases. As a result, rich-lean separation appears again at the outlet.

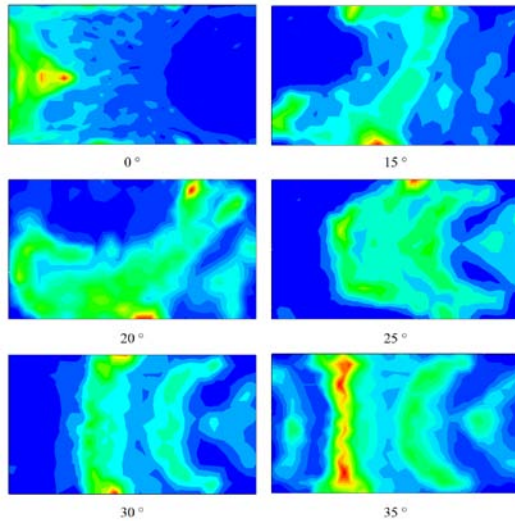


Fig. 2 The outlet concentration distribution of different angle

**Impact of bias block’s location**

Figure 3 shows pulverized coal concentration distribution in the export of the six cases with L=0, 50, 100, 150, 200, 250mm (α = 20°). It can be seen from the figure, when the bias block angle is 20°, pulverized coal concentration of different L burners is relatively uniform in the export and there is no great difference. When the bias block is near from the elbow, there is a small pulverized coal concentrated region in the export. As the distance between the bias block and elbow

increases, the small pulverized coal concentrated region moves to the right, and has a decreasing trend. Distance continues to increase, the small pulverized coal concentrated region turns to be larger again and over the midline. When the bias block is near from the elbow, the rich side of the pulverized coal is moving closely to the elbow and will be bumped on the bias block before the direction of velocity shifts, then the blend of the rich side and lean side will be weakened. With a longer distance, the rich side of the pulverized coal is bumped by bias block and the flow direction shifts to the lean side; the two flows mixture and the outlet concentration distribution becomes uniform. The distance becomes much larger, that is, the distance to the export decreases, the rich side and lean side have not had enough time to fully mixed before reaching the exit, which results in nonuniform coal distribution and less effective anti-bias.

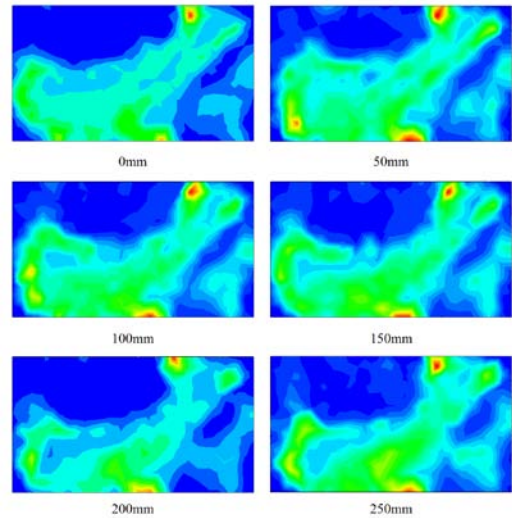


Fig. 3 The outlet concentration distribution of different location

**Rich-lean separation factor**

In order to study the rich-lean separation effect of burners with and without bias block, divide the burner outlet section into two regions averagely and define the pulverized coal concentration points ratio of rich side and lean side as rich-lean separation factor. The rich-lean separation factor is directly promotional to separation effect,

$$\Phi = \frac{\iint_{A_r} \rho dA}{\iint_{A_l} \rho dA}$$

where A<sub>d</sub> is the area of rich side region, A<sub>l</sub> is area of lean side region, and ρ is coal density.

Table 3 shows the rich-lean separation factors of thirty different cases researched. The closer to 1 the rich-lean separation factor is, the more uniform the outlet coal distribution is. Table 2 shows that, when α = 25° L = 150mm, the rich-lean separation factor is the closest to 1 and pulverized coal distribution of the burner outlet is the most uniform.

Table 3 Rich-lean separation factor

$\alpha \backslash L$	0mm	50mm	100mm	150mm	200mm	250mm
15°	2.3749	2.2281	2.2801	2.2448	2.2596	2.2908
20°	1.1535	1.1718	1.037	1.1395	0.9283	1.0231
25°	0.9733	0.9301	1.0085	1.0019	0.8468	0.8452
30°	0.8026	0.8589	0.8356	0.6573	0.7113	0.6504
35°	1.2693	1.1849	1.0346	1.0793	0.9909	0.9019

**Resistance Analysis**

Figure 4 shows the pressure drop of the thirty different cases. It can be seen that as the angle increases, the pressure drop across the burner gradually become larger, whereas it does not change significantly with distance; it suggest that the bias block angle changes is the main reason of generating resistance. Considering both pulverized coal distribution situation and resistance, when  $\alpha = 25^\circ$   $L = 150\text{mm}$ , the distribution of pulverized coal of the burner outlet is the most uniform and the resistance is not large.

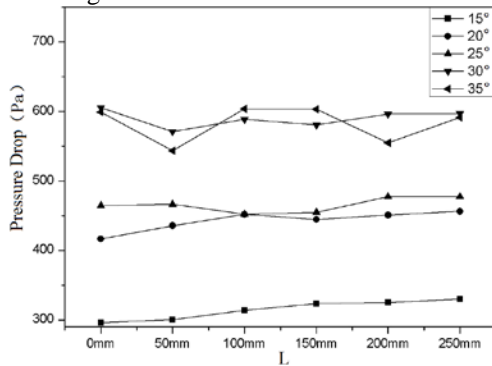


Fig. 4 Pressure drop of burner import and export

**CONCLUSIONS**

In this paper, the gas-solid flow in a special structured burner of a power plant has been simulated. The following conclusions can be made:

- (1) Installing a bias block in the pulverized coal rich side behind the bend could achieve the effect of uniform concentration distribution at primary air outlet and could make sure that the rich side of pulverized coal does not get close to the wall.
- (2) As the bias block's angle increasing, the distribution of pulverized coal tends to be uniform and the coal distribution of the burner outlet gradually tends to be uniform. Bias block angle continues to increase, the distribution of coal appeared high concentration region and concentration core again. As the distance between bias block and elbow increases, the overall distribution of pulverized coal of burner exit moves to the right.
- (3) Relative to the distance, the bias block angle changes is the main reason of generating resistance.
- (4) When  $\alpha = 25^\circ$  and  $L = 150\text{mm}$ , the distribution of pulverized coal of the burner outlet is the most uniform and the resistance is not large, which could satisfy the

good anti- bias effect and moderate resistance loss at the same time.

**ACKNOWLEDGEMENTS**

The present work is supported by the National Natural Science Foundation of China (No. 51076105) and the National Natural Science Foundation of China (No. 51129602)

**REFERENCES**

- [1] Li Y.P., Wu J.B., Ren T., Li G.N., Zhou, H. , Cen, K.F., "The effect of primary air duct elbow on gas-solid flow of swirling burner outlet," Energy Engineering, No. 2, (2011),:6-8
- [2] Yang, M., Guo, C.S., Zhang, Y.W., Kang Z.Y., "Concentration Distribution Research of a Special DC Pulverized Coal Burner," Proceedings of the ASME 2011 International Mechanical Engineering Congress &Exposition, (2011), Denver, CO.
- [3] Zhou, H., Cen, K.F., Fan, J.R., Chi, Z.H., Jiang, X. "A Simulation Study on the Separating Performance of an Impact Type Fuel Rich-Lean Burner Affected by the Elbows," Proceedings of the CSEE, Vol. 23, No.1, (2003) 132-135
- [4] Jing, Y.Y., Qi, Y.X., Zhao, Q.B., Qi, X.W., Wang, B.S., "Numerical Simulation of Gas-Solid Two-phase Flow in Horizontal Rich/Lean Pulverized Coal Burners," Power Engineering, Vol.25, No.1, (2005) 65-67
- [5] Jiang, X., Chi, Z.H., Zhou, H., Xu, Z., Chen, L.H., Cen, K.F., "A new burner with pulverized coal separator," Thermal Power Generation, No.2, (1998) 4-7
- [6] Xu, J.R., Yao, Q., Cao, X.Y., Cen, K.F., "Numerical Simulation of Gas solid Two Phase Flow in Pulverized Coal Boiler of Bumping Separation and Adjustable Concentration," Journal of Combustion Science and Technology, Vol.5, No.4, (1999)422-426
- [7] Xia, Z.H., Zhang, X.Y., Fan, J.R., Cen, K.F., " Numerical Simulation on the Rich/Lean Pulverized Coal Burner," Journal of Combustion Science and Technology, Vol.6, No.3, (2000) 214-217
- [8] Chi, Z.H., Jiang, X., Cen, K.F., Han, Z.L., Kong, G, Li, F.M., "Application of Rich/Lean Pulverized Coal Burner in Xiaoshan Power Plant," Boiler Technology, No.2,(1996)5-9
- [9] Yan Z.R., " Effect of a Bumping Separator(BS) on Rich-Lean Flow Separation and NOx Emission in the Spout of a Pulverized Coal Rich-Lean Burner(PCRLB)," Journal of Power Engineering, Vol.26, No.5, (2006) 641-645
- [10] Cen, K.F. and Fan, J.R., "Engineering theory and gas-solid multiphase flow calculations," Zhejiang University Press, Hangzhou: 1990
- [11] Morsi, S.A., and Alexander, A. J., "An Investigation of Particle Trajectories in Two-Phase Flow Systems," Fluid Mech, Vol. 55, (1972) 193-208